Drag Reduction by Polymers

→ These two lectures explore the physics of drag reduction in (mainly) turbulent pipe flow by small amounts of polymer additives.

→ Caveat Emptor:

- remains an open problem - no clean solution

- some facts, ideas and many speculations abound

- cannot be balanced, inclusive or up to date in short discussion

→ reflects my personal views/perspective

but:

- the subject is interesting, fun and sometimes amazing

- has captivated several 'Greats'

- you will learn something!

— Outline

① → Drag and Drag Reduction in Pipe Flow

② → A Primer on Polymers in Dilute
    Solutions

  cf.   P.-G. deGennes   "Scaling Concepts in Polymer
                            Physics"

       → on short list of <u>great</u> physics books

also { M. Doi, S. Edwards, " Theory of Polymer Dynamics"

      { M. Doi , " Soft Matter Physics"

    R. B. Bird, et.al. " Dynamics of Polymeric
                       Liquids, Vol. I, II".

③ → Some Ideas from the Greats

④ → A Continuum Model (which looks
        familiar)

⑤ → More Ideas on Poly-Hydro Turbulence

⑥ → Related Observations / Thoughts.

① Drag and Drag Reduction in Pipe Flow

→ Recall Drag → ala' Prandtl

$\not\sqcup \not\sqcup \not\sqcup \not\pi$ core

———————— inertial sublayer
———————— viscous sublayer

← Δp →

L - O - W

$\Delta p \, \pi a^2 = \pi_{x,z} (2\pi a L)$

$\pi = \rho u_*^2$

$\rho u_*^2 = -\nu_T \dfrac{\partial \langle u \rangle}{\partial x}$

$\nu_T = u_* \times$
$\quad\quad\quad\searrow$ mixing length

key : – Momentum transport $\leftrightarrow$
turbulent stress

– no-slip B.C.

– scale covariance between
$x_{SL} = \nu / u_*$ and a.

Result: $\langle u \rangle = u_* \ln (x / x_{SL})$

and $\quad \epsilon = u_*^3 / x$

$\rightarrow \begin{cases} \text{turbulent} \\ \text{dissipation strongest} \\ \text{at } x = x_{SL} + \end{cases}$

$\rightarrow$ strongest
shears, etc.

Score: — λ vs Re plot

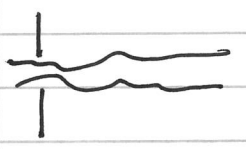— $\lambda = \dfrac{2a \Delta p / L}{\frac{1}{2} \rho U^2}$

But:

→ Drag Reduction Happens with Polymers!!

— c.f. → w/wo comparison by NYFD circa 1969

→ nb: unclear ~~xxxx~~ whether injection or lining of hoses.

→ Compare jet w/wo :

— observe absence with of droplets, small scale structure

— "Filaments" with

N.B. Structure of turbulent jet with polymer additives is strikingly different from w/o.

more rapidly than in turbulent flow.

Figure 32 shows a logarithmic graph of λ as a function of R. The steep straight line corresponds to laminar flow (formula (43.6)), and the less steep curve (which is almost a straight line also) to turbulent flow. The transition from the first line to the second occurs, as the Reynolds number increases, at the point where the flow becomes turbulent; this may occur for various Reynolds numbers, depending on the actual conditions (the intensity of the perturbations). The resistance coefficient increases abruptly at the transition point.

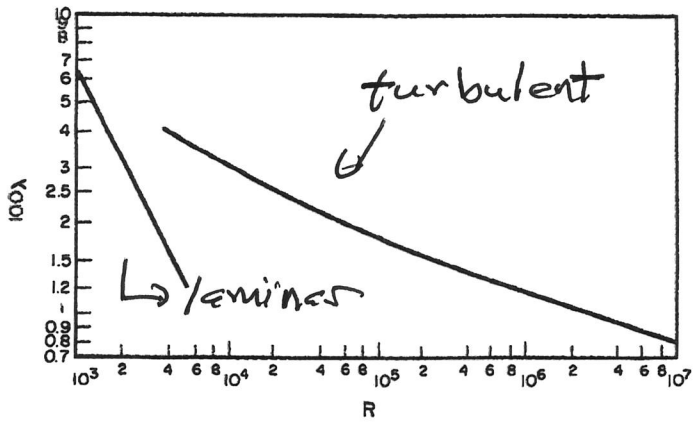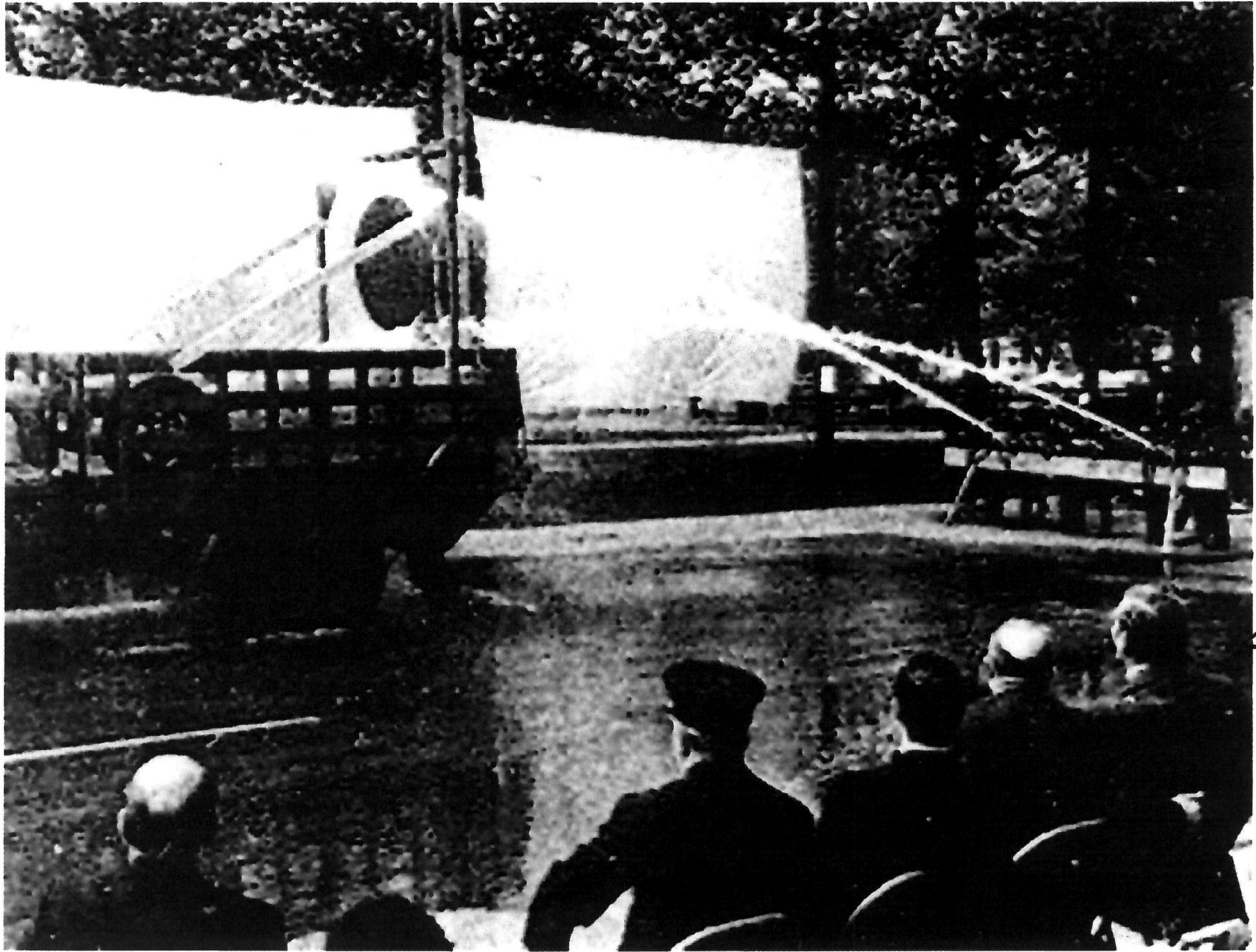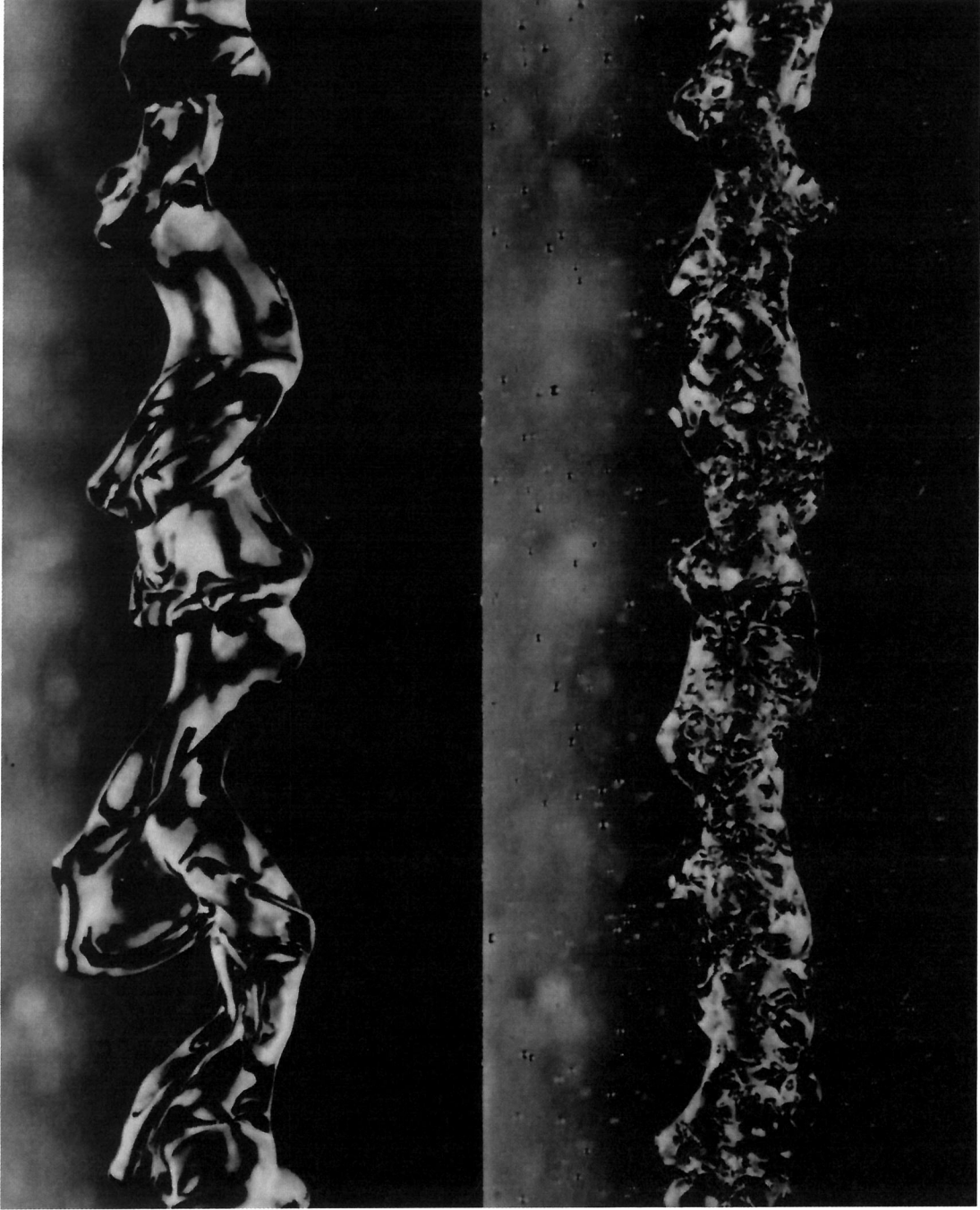$$\lambda \sim \frac{\Delta p}{\rho u^2 / 2}$$

FIG. 32   Re

Fire hose demonstration.
New York City, 1969

Mayor
J.V.L.

w/wo   polymers.

jet comparison

W

⤷ droplets fragment

W/O

small sidestrut.

from Bird, et. al.

4c.

4d.

Jet comparison — Further downstream
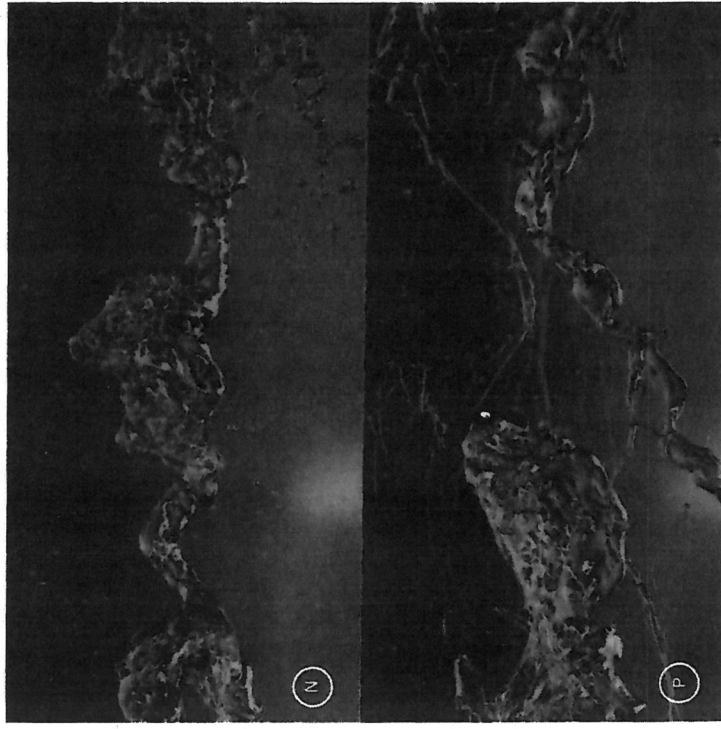
Jet break-up
w/o

W
[note Filament]

from Berg et al./Pld

FIGURE 2.7-4. High-speed photographs taken 2 m from the orifice of the same two jets shown in Fig. 2.7-3. [Reproduced from photographs courtesy of J. J. Taylor, Independent Consultant, Santa Barbara, CA, and J. W. Hoyt, Department of Mechanical Engineering, San Diego State University.]

→ Drag Reduction in Pipe Flow

↪ the 'marquee problem'.

Now :

→ few ppm of polymers sufficient to significantly reduce drag

→ no impact on laminar drag curve!

→ suggests only turbulence can access beneficial aspects of polymer solution

→ drag reduction increases with concentration (though occurs for 5 ppm!).

→ some evidence of a "maximal" drag reduction i.e. @ parallel to, but displaced from, laminar curve.

N.B.: P.S. Virk, AI Ch.E Journal Vol. 21, #4 625 (1975)

is an old ▓ but excellent review!.

→ good job on basics of drag reduction phenomenology.
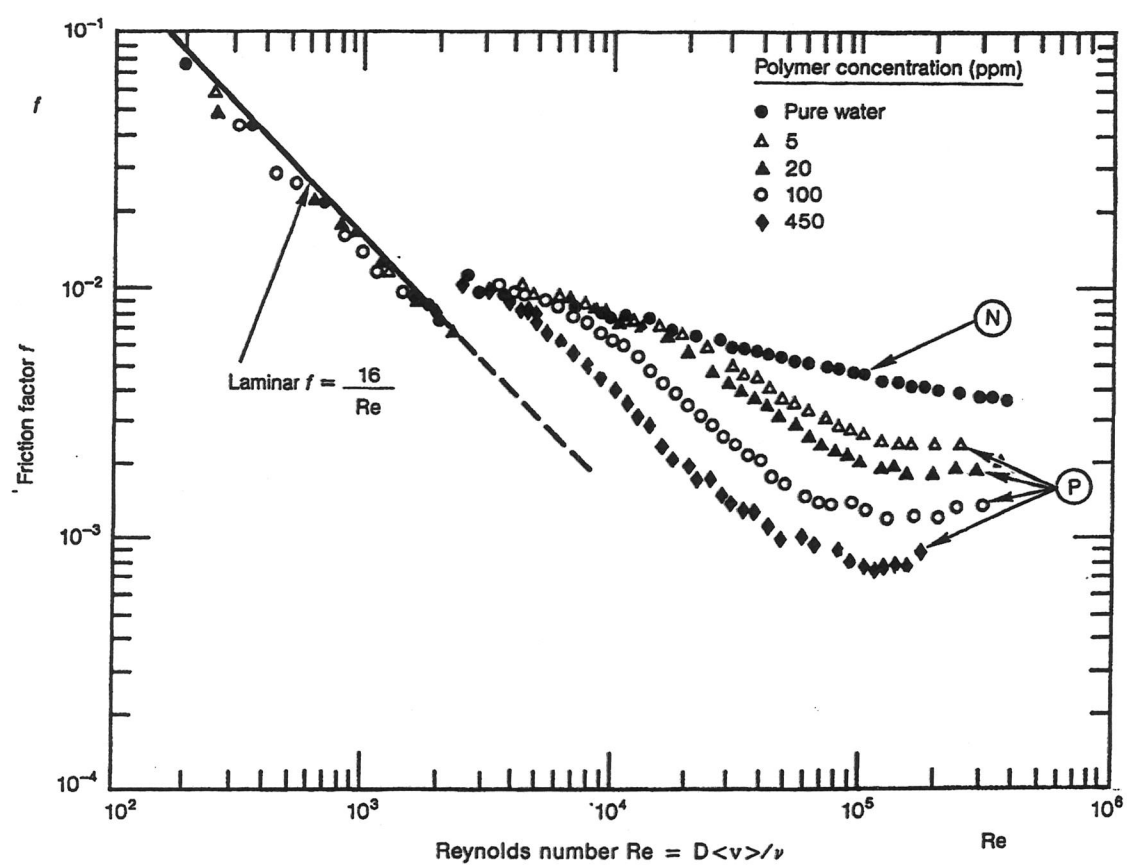
Figure 1-1. Plot of the "friction factor" defined in the text as a function of Reynolds number for turbulent water flowing in a pipe with various concentrations of PEO. Points labelled "N" are with no polymer additives, while points labelled "P" have polymers in varying concentrations; from Ref. [2]

→ few PPM sufficient

→ laminar friction factor unchanged.

→ drag reduction increases with concentration

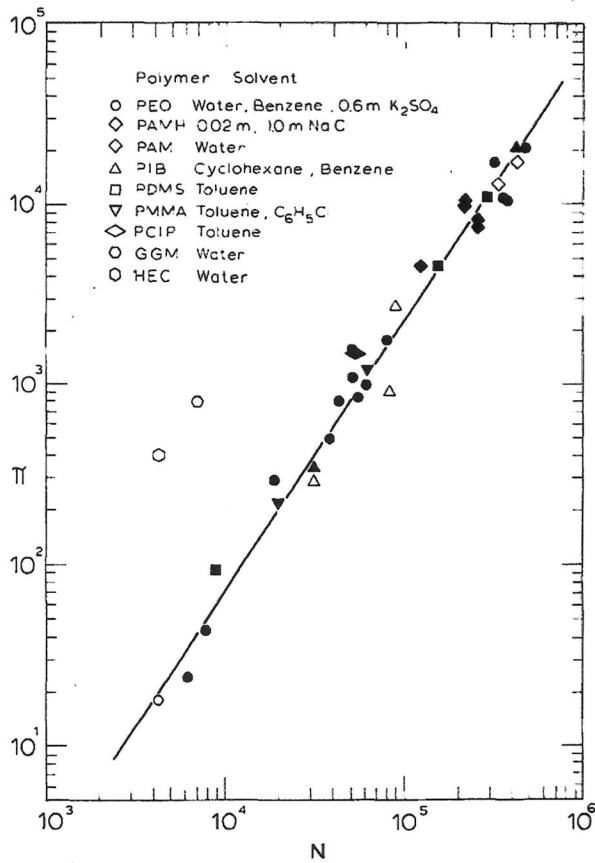→ "maximal" drag reduction

5

(Virk)

Fig. 6. Relationship between intrinsic slope increment and number of backbone chain links for some linear, random-coiling macromolecules. Solid line corresponds to a slope modulus $\kappa = 70 \times 10^{-6}$. Data from Table 2.

shown in Figure 7, despite differences among their trajectories at the lower $Ref^{1/2}$. Perusal of the experimental details associated with the data of Figure 7 will show that, besides being independent of pipe diameter, the asymptotic maximum drag reduction is strikingly insensitive to polymer species, molecular weight, and concentration, which contrasts with the pronounced dependence of drag reduction on these polymeric parameters witnessed in the preceding polymeric regime. The maximum drag reduction asymptote has been widely observed and seems to be a fundamental feature of the drag reduction phenomenon. Some recent results are presented in Figure 8, P-K coordinates, in which the solid line labeled *mdr asymptote* corresponds with Equation (4) of the text. The magnitudes of maximum drag reduction are worth noting. At $\overline{Ref}^{1/2} = (300, 1000, 3000)$, the respective fractional flow enhancements relative to Newtonian are $S_F = (0.54, 1.12, 1.49)$; at the corresponding $Re = (4.4 \times 10^3, 2.5 \times 10^4, 10^5)$, the respective fractional drag reductions relative to Newtonian are $R_F = (0.52, 0.73, 0.80)$.

1.1.6 Transition. The transition from laminar to turbulent flow with dilute polymer solutions can be appreciated by observing first some of the gross flow trajectories depicted in Figures 1 and 7. In Figure 1, the polymer solution shows the laminar, Newtonian, and polymeric regimes, an LNP trajectory, while in Figure 7 we observe two LPM trajectories, for the 38 wppm PAM solution (hollow squares) and for the 1000 wppm PEO solution (hollow diamonds), and two LM trajectories, for the 300 wppm PEO solution (triangles) and the 100 wppm PAM solution (solid squares). Evidently, the existence of one laminar and three turbulent flow regimes makes for three possible laminar-to-turbulent transitions, which we designate $L \rightarrow N$, $L \rightarrow P$, $L \rightarrow M$, respectively. These seem to have the following characteristics:

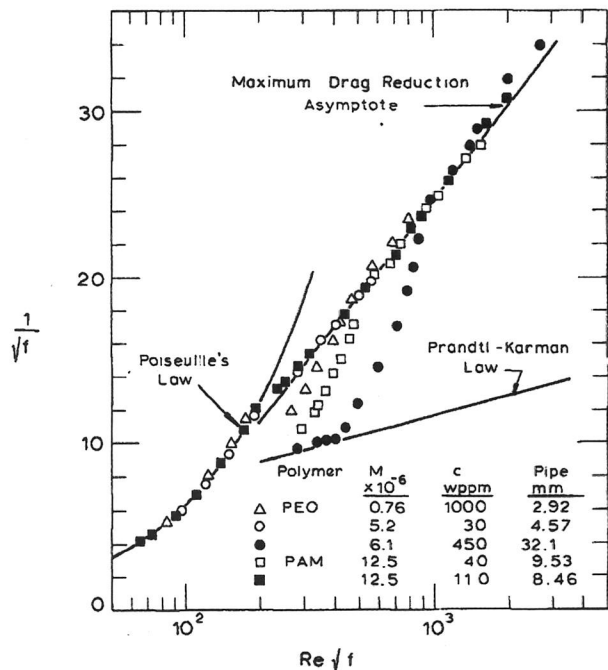1. $L \rightarrow N$. The transition with polymer solution is pre-

Fig. 7. Gross flow trajectories exhibiting maximum drag reduction. In all cases solvent was distilled water, temperature 25 C. (Polymer, $M \times 10^{-6}$, c wppm, d mm) as follows: (PEO, 0.76, 1000, 2.92), (PEO, 5.2, 30, 4.57), (PEO, 6.1, 450, 32.1), (PAM, 12.5, 40, 9.53), (PAM, 12.5, 110, 8.46).
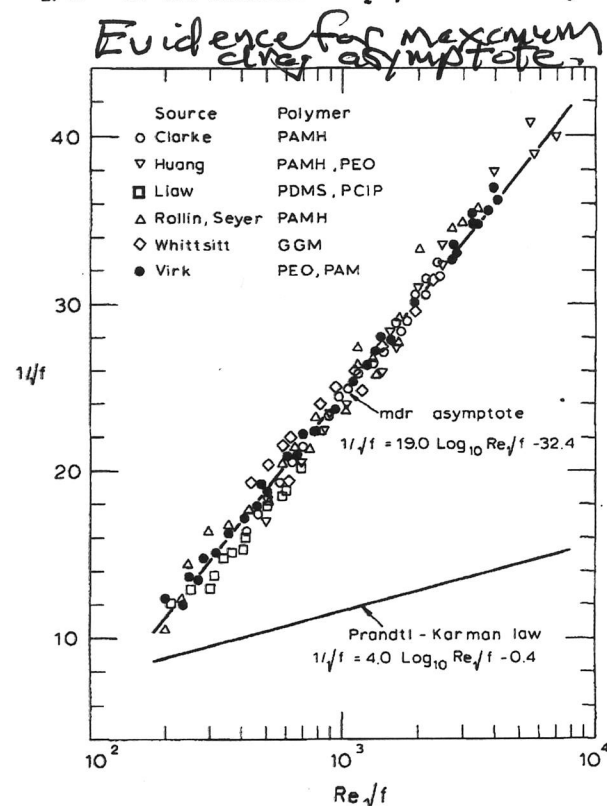
Fig. 8. The maximum drag reduction asymptote in pipe flow of polymer solutions. See Table 4 for experimental details.

Note: Pipe diameter and other details irrelevant.

Significant: Critical stress!

→ There is a critical wall stress (ρU_*^2) for onset of drag reduction

and

→ Wall stress inversely related to radius of gyration of polymers.

← R_g →

Structure of Profiles:

→ drag reduction does not change viscous sublayer structure

i.e. viscous flow does not 'activate' the polymer

→ drag reduction leaves core of inertial sublayer and core unchanged

BUT:

Solution viscosities are generally so close to solvent that shear thinning, which almost all polymer solutions exhibit to some extent at high enough shear rates, has little discernible effect on the gross flow. In fully turbulent pipe flow, dilute polymer solutions exhibit three distinct regimes which are, in order of increasing flow rate:

1. A regime without drag reduction in which the friction factor relation is the same as for solvent, that is, the usual Prandtl-Karman (or Blasius) law for Newtonian turbulent flow

$$f^{-1/2} = 4.0 \log_{10} Re f^{1/2} - 0.4 \tag{2}$$

2. A regime with drag reduction in which the friction factor relation depends upon the nature of the polymer solution. Anticipating later results, an approximate relation for this regime is

$$f^{-1/2} = (4.0 + \delta) \log_{10} Re f^{1/2} - 0.4 - \delta \log_{10} \sqrt{2} dW^{\bullet} \tag{3}$$

where δ, $W^{\bullet}$ are polymer solution parameters.

3. An asymptotic regime of maximum possible drag reduction in which the friction factor relation is insensitive to the polymer solution employed, being, universally,

$$f^{-1/2} = 19.0 \log_{10} Re f^{1/2} - 32.4 \tag{4}$$

The foregoing will respectively be termed the Newtonian (N), polymeric (P), and maximum drag reduction (M) regimes, the laminar (L) regime having been noted first. Laminar to turbulent transition is not well detected by gross flow studies and therefore only a brief description will be given in Section 1.1.6 after the turbulent flow regimes have been considered.

1.1.2 Polymeric Regime. Aspects of the polymeric regime are illustrated in Figures 2a to 2d using P-K coordinates with abscissae $Re_s f^{1/2}$, all based on solvent viscosity.

The effect of pipe diameter is shown in Figure 2a which contains data for solvent (hollow points) and the same polymer solution in each of three pipes, of inside diameters respectively 2.92, 8.46, and 32.1 mm. Two features merit attention. First, the onset of drag reduction in the three cases occurs at $Re_s f^{1/2 \bullet} \simeq 400, 1100,$ and 4000, the ratio of which, 0.36:1.0:3.6, closely approximates the ratio of pipe diameters, 0.35:1.0:3.8. Thus, regardless of pipe size, the given polymer solution reduces drag only after a certain wall shear stress $T_w^{\bullet} \simeq 7.0$ N/m² has been exceeded. Second, it will be noticed that, after onset, the polymer solution data describe approximately straight lines which have much the same slope in all pipes. The difference between polymer solution and solvent slopes, called the *slope increment*, is in this case $\delta = 11 \pm 2$.

The effect of polymer concentration is shown by Figure 2b which displays data taken in the same pipe for solutions of the same polymer ranging in concentration from 50 to 1000 wppm. For clarity, solvent (distilled water) data have been omitted, being replaced by solid lines representing the Prandtl-Karman law (2) to which they closely adhered; also, ordinates have been shifted upward in an obvious way for each successive set of data, and straight lines have been drawn through the polymer solution points after onset. In each case it can be seen that the onset of drag reduction occurs at a rather well defined $Re_s f^{1/2 \bullet}$. Further, in all four solutions, spanning a 20-fold concentration range, onset occurs at much the same $Re_s f^{1/2 \bullet} = 1150 \pm 100$. Thus, the onset wall shear stress is essentially independent of polymer concentration. After onset *the polymer solution data are quite well approximated by the indicated straight lines, the slopes increasing with increasing concentration such that the slope increment is* $\delta = (4.3, 6.9, 11.7, 18.5)$ for $c = (44, 100, 300, 940)$ wppm, respectively. Scrutiny of these results will reveal

that δ varies approximately as the square root of polymer concentration with $\delta/c^{1/2} = 0.65 \pm 0.05$.

The effect of polymer molecular weight is illustrated in Figure 2c, using data taken in the same pipe with distilled water solutions of various homologous PEO polymers ranging in molecular weight from 0.1×10^6 to 8×10^6. It is apparent that, as molecular weight is increased, the

Pipe diameter irrelevant

Fig. 2a. Aspects of the polymeric regime: Effect of pipe diameter. Pipe I.D. 2.92, 8.46, and 32.1 mm, temperature 25 C, solvent distilled water, polymer solution PEO, $M = (0.66 \pm 0.10) \times 10^6$, $c = 250 \pm 50$ wppm.

Fig. 2b. Aspects of the polymeric regime: Effect of concentration. Pipe I.D. 8.46 mm, temperature 25 C, solvent distilled water, polymer PEO, $M = 0.57 \times 10^6$, $c = 44, 100, 300, 940$ wppm.
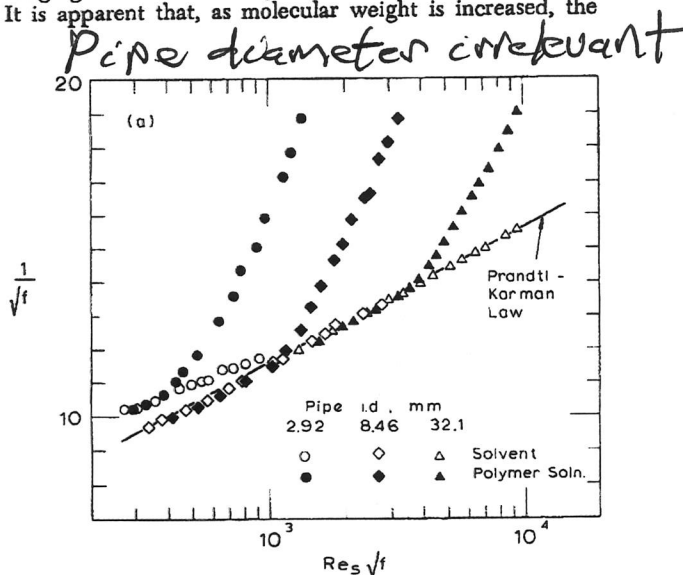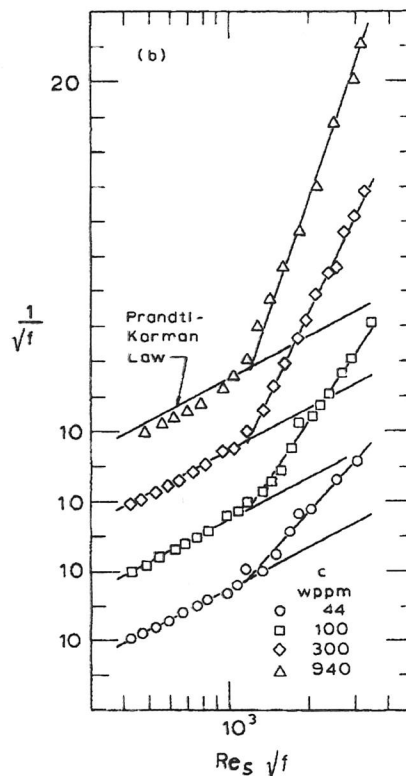
Virk, 75.
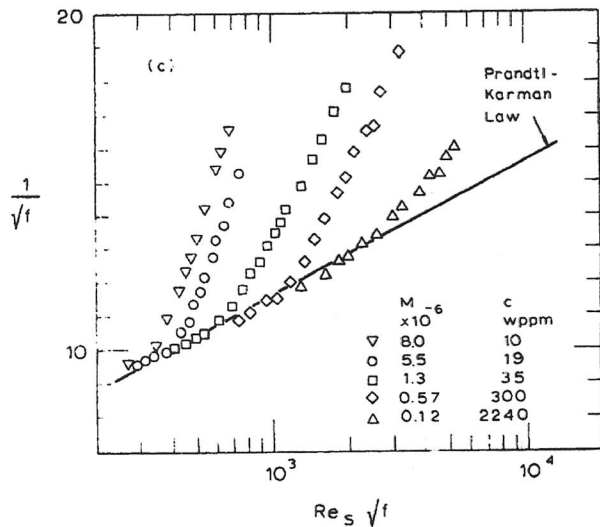
Benefits of higher concentration

Fig. 2c. Aspects of the polymeric regime: Effect of molecular weight. Pipe I.D. 8.46 and 9.45 mm, temperature 25 C, solvent distilled water, polymer PEO, (M × 10^{-6}, c wppm) as follows: (8.0, 10), (5.5, 10), (1.3, 35), (0.57, 300), (0.12, 2240).
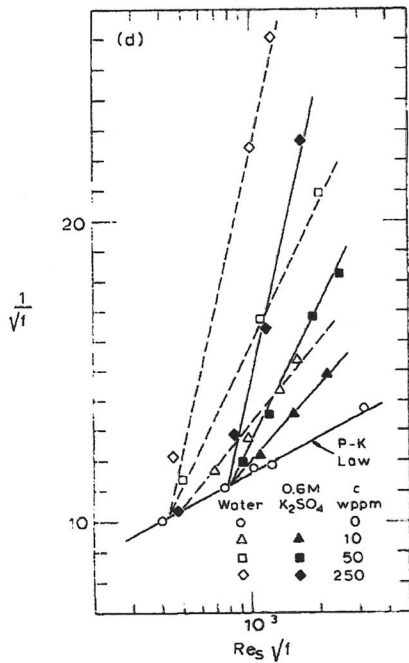

Fig. 2d. Aspects of the polymeric regime: Effect of polymer coil size (data from Pruitt, Rosen, and Crawford 1966). Pipe I.D. 4.57 mm, temperature 22 C, solvents water and 0.6m K$_2$SO$_4$, polymer PEO, M = 0.8 × 10^6, c = 10, 50, 250 wppm.

onset of drag reduction occurs at lower $Re_s f^{1/2 *}$, and strikingly lower concentrations are required to yield a given slope increment. Molecular weight thus strongly influences the effectiveness of a polymer in reducing drag and, speaking qualitatively, T_w^* varies inversely and δ directly as M.

The effect of polymer random coil size in solution is shown in Figure 2d, using data derived from Pruitt, Rosen, and Crawford (1966), who studied drag reduction by the same PEO polymer in water, a good solvent, and in 0.6m K$_2$SO$_4$, a poorer solvent. From their reported intrinsic vis-

cosities of the polymer in these two solvents, R_G is estimated to be 96 nm in water and 65 nm in 0.6m K$_2$SO$_4$. In Figure 2d, all of the data shown were obtained in the same pipe; the bottom-most solid line represents the Prandtl-Karman law, polymer concentrations are distinguished by symbols, water solution data (hollow) are faired through by broken lines, and 0.6m K$_2$SO$_4$ solution data (solid) by light continuous lines. It is evident that the change in solvent from water to 0.6m K$_2$SO$_4$ shifts the onset of drag reduction from $Re_s f^{1/2 *} \simeq 500$ to $Re_s f^{1/2 *} \simeq 800$ but does not appreciably alter the slopes exhibited by the polymer solutions after onset. Thus, a decrease in the dimensions of a macromolecular random-coil in solution increases the onset wall shear stress but does not much affect the slope increment.

The effect of solvent viscosity on drag reduction is still uncertain, fragmentary evidence (Section 2) suggesting that T_w^* is independent of viscosity.

1.1.3 Onset. In summary, the onset of drag reduction occurs at a rather well-defined onset wall shear stress T_w^*. For a given polymer solution, T_w^* is essentially the same in pipes of different diameters. For solutions of a given polymer-solvent combination, T_w^* is approximately independent of polymer concentration. And onset depends on the polymer random-coil size in solution, with T_w^* increasing as R_G decreases. The onset of drag reduction implies incipient interaction betwen the turbulent flow and the polymer molecule in solution and, among experimentally accessible quantities, T_w^* and R_G are respectively the flow and polymeric parameters most relevant to onset. The relationship observed between T_w^* and R_G in the pipe flow of PEO solutions is indicated in Figure 3, log-log coordinates. Amid scatter, T_w^* varies as an inverse 2 to 3 power of R_G. The solid line in the figure has been drawn with slope −3 and represents the data within a factor $2^{\pm 1}$ over a 500-fold
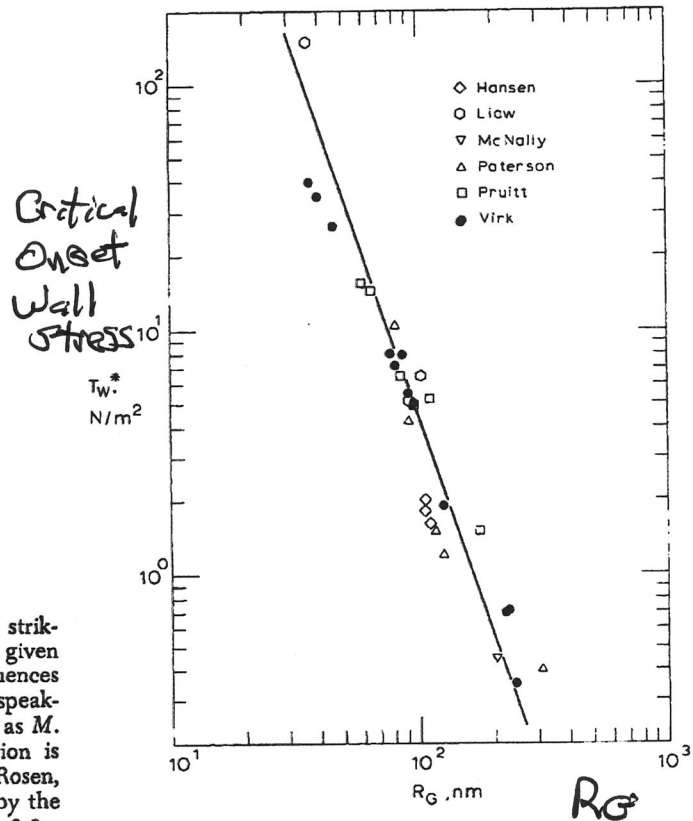

Fig. 3. Onset results for polyethyleneoxide solutions. Solid line corresponds to an onset constant $\Omega_T = 4.4 \times 10^6$. Data from Table 2.
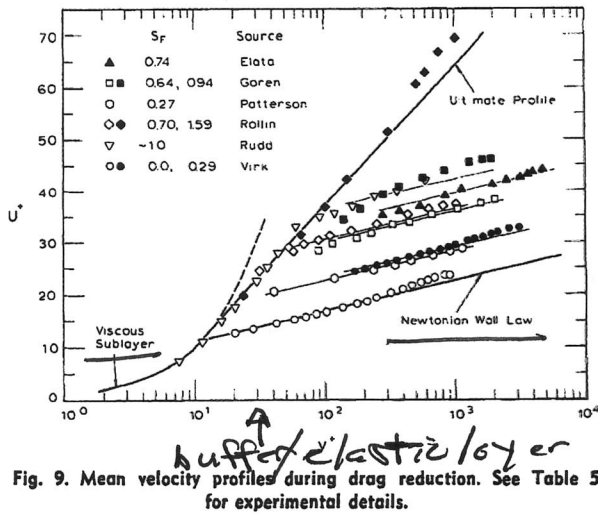
Fig. 9. Mean velocity profiles during drag reduction. See Table 5 for experimental details.

[handwritten: buffer elastic layer]

cisely the same as in the usual Newtonian case (Rotta, 1956). There is a critical Reynolds number Re_{tr}, which marks the beginning of a regime of intermittent laminar and turbulent slugs that finally terminates in fully turbulent flow.

2. $L \rightarrow P$. This transition is very similar to Newtonian, with much the same critical Reynolds number, turbulent slug lengths, and growth rates. However, the turbulent slug formation frequency seems to be greater than Newtonian and increases with the drag-reducing ability of the polymer solution.

3. $L \rightarrow M$. In this transition, exhibited by very strongly drag-reducing solutions, velocity fluctuations are apparent at $Re \simeq 1500$, decidedly lower than the Newtonian Re_{tr} = 2000, but intermittency cannot be readily discerned.

The kind of transition observed apparently depends upon whether or not the onset of drag reduction occurs in the turbulent slugs which appear for $Re > Re_{tr}$. Also, Re_{tr} in polymer solutions appears always to be equal to or less than Re_{tr} in solvent; in no case do the polymer solutions delay transition. It should be pointed out that the preceding summarize our data for triggered (that is, high inlet disturbance) transition in pipes (Ohara, 1968) and agree substantially with the conclusions of Paterson and Abernathy (1972), but are contrary to those of Castro and Squire (1967), Giles and Pettit (1967), and White and McEligot (1970).

1.2 Mean Velocity Profiles

1.2.1 Law of the Wall. Representative mean velocity data are shown in Figure 9, a law of the wall plot with nondimensional coordinates of U^+ versus log y^+. On the figure, fractional flow enhancement S_F is used to denote the drag reduction. Other experimental details corresponding to the data shown in Figure 9 are contained in Table 5 of Section 2, casual perusal of which will indicate the various pipe sizes, polymers, and concentrations used. The three heavy solid lines in Figure 9 respectively represent the viscous sublayer

$$U^+ = y^+ \tag{7}$$

the Newtonian law of the wall

$$U^+ = 2.5 \ln y^+ + 5.5 \tag{8}$$

and the ultimate profile

$$U^+ = 11.7 \ln y^+ - 17.0 \tag{9}$$

the last arising from the maximum drag reduction asymptote as explained later. Turning to the data, it is seen that,

at zero drag reduction (Virk $S_F = 0$), the polymer solution profile adheres to the Newtonian wall law. At low drag reduction (Patterson $S_F = 0.27$, Virk $S_F = 0.29$), the polymer solution profiles are shifted upward from but parallel to the Newtonian wall law. The parallel upward shift, called (after Oldroyd, 1948) the *effective slip* S^+, increases with increasing drag reduction (Goren $S_F = 0.64$, Rollin $S_F = 0.70$, Elata $S_F = 0.74$). At still higher drag reductions (Goren $S_F = 0.94$, Rudd $S_F = 1.0$), an upward shifted region of roughly Newtonian slope is still discernible, but at the lower y^+, toward the wall, the profiles exhibit a slope significantly greater than Newtonian. Finally, at maximum drag reduction conditions (Rollin $S_F = 1.59$), the entire profile is approximately semilogarithmic with a slope $\simeq 12$, about five times that of the Newtonian wall law.

1.2.2 Velocity Defects. A portion of the mean velocity data considered in Figure 9 are shown again in a velocity-defect plot, Figure 10, on arithmetic coordinates of the velocity defect $U_1^+ - U^+$ versus radius-normalized distance from the wall ξ. This is the conventional, and sensitive, method of displaying mean velocity profiles relative to the mean velocity on the pipe axis, the arithmetic abscissa emphasizing the central region of the pipe. The solid line represents the Newtonian velocity defect law including a small, but significant, wake correction as given by Hinze (1959); solvent data reported by the investigators quoted in Figure 10 were all in close agreement with this line but are omitted for clarity. Of the results with polymer solutions, those at the lower, but nevertheless considerable, drag reduction (Virk $S_F = 0.29$, Goren $S_F = 0.64$, Rollin $S_F = 0.70$) show velocity defect profiles identically the same as Newtonian for $1.0 > \xi >$ 0.05. As drag reduction is increased (Goren $S_F = 0.94$), the velocity defect remains Newtonian toward the axis $1.0 > \xi > 0.2$ but is greater than Newtonian toward the wall $\xi < 0.2$. At maximum drag reduction (Rollin $S_F = 1.59$), the velocity defect exceeds Newtonian over the entire pipe cross section. Evidently, the mean velocity profiles retain a Newtonian velocity defect structure over a region, $1 > \xi > \xi_e$, which we will call the *Newtonian plug*, the inner (wall-ward) boundary of which ξ_e moves progressively toward the pipe axis $\xi = 1$ with increasing drag reduction. Too, the Newtonian defect structure is retained despite absolute velocities significantly, and by various amounts, higher than Newtonian as already seen in the parallel upward shifts exhibited by these profiles in Figure 9.

1.2.3 Velocity Profile Zones. The characteristic feature of mean velocity profiles during drag reduction seems to be the appearance of a region, lying somewhere between the viscous sublayer and the outer Newtonian plug, in which the mean velocity increases to above Newtonian by an amount S^+. While such a region, which we will call the *elastic sublayer*, can actually be seen in the data of Rudd (1969), roughly $15 < y^+ <$ 60 in Figure 9, other profiles at lower drag reduction do not extend close enough to the wall to make it visible. However, from the pipe axis inward, these profiles are observed to be parallel-shifted upward from Newtonian by S^+, and from the wall outward we have the conviction that, in polymer solutions as in Newtonian fluids, the profiles must start out along a viscous sublayer and, hence, between the viscous sublayer and the Newtonian plug must be a region, characteristic of drag reduction, across which the effective slip occurs. Mean velocity profiles during drag reduction have thus three zones from the wall outward: (1) a viscous sublayer, (2) an elastic sublayer, characteristic of drag reduction, across which the effective slip S^+ occurs, and (3) a Newtonian plug which retains the Newtonian defect structure though absolute velocities

— Slip Layer // Buffer Layer forms
with polymers.

$\frac{i.e.}{\overline{\tau_{in}}}$ inertial   buffer/slip ↓

viscous
in

strt line flux
n.b: Prandtl worked
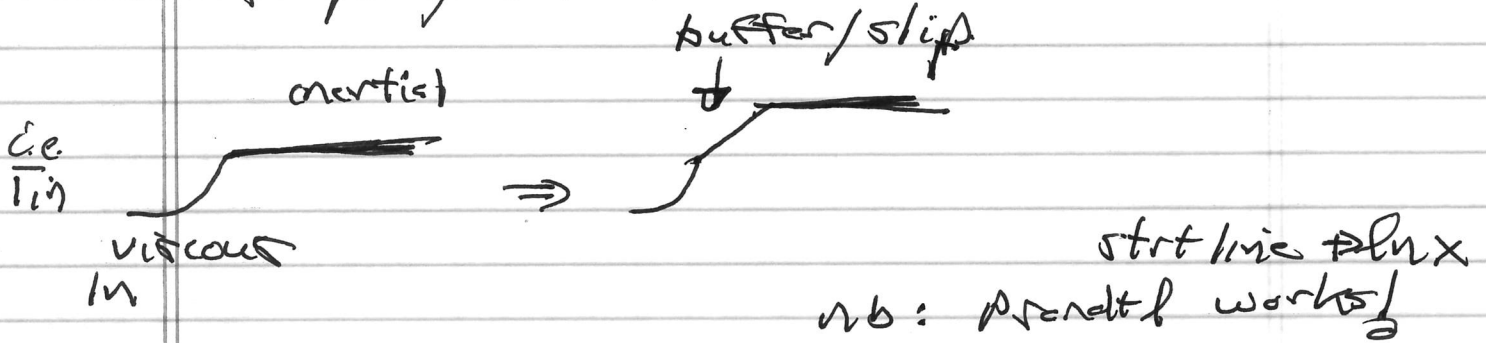
Note slip/buffer layer:

→ steepens local ∇U

→ necessarily reduced local momentum
transport
⟷ Momentum transport barrier Ⓣ

→ slip layer expands with c,
approaching ultimate profile.

— Re: Momentum transport barrier,

— momentum flux is local $\langle UV \rangle$

— stress drops with polymer
additive)

— $c(u,v) = \langle uv \rangle / |u||v|$ drops

with polymers ⇒ effect on
cross-phase.

agrees with Logan's results (Figure 11b). Concerning the variation of turbulent intensity profiles with drag reduction, the data of Logan ($S_F \simeq 0.4$) and Rudd ($S_F \simeq 1.0$) respectively yield a ratio of maximum axial intensity in polymer solution to that in solvent ($u_{max,p}'^+/u_{max,n}'^+$) of 1.3 and 1.8, while in the pipe core the regions where u'^+ is the same as in solvent are $1.0 > \xi > 0.4$ and $1.0 > \xi > 0.6$, respectively. At (or near) maximum drag reduction, there is only uncertain information from streak photography (Seyer and Metzner, 1969; Arunachalam, Hummel, and Smith, 1972), which suggests that ($u_{max,m}'^+/u_{max,n}'^+$) is 2.0 to 2.5.

1.3.2 Reynolds Stress and Correlation Coefficient. Reynolds stress data reported by Logan (1972) and *u-v* correlation coefficients calculated therefrom are shown in parts a and b, respectively, of Figure 12, using a common wall-region abscissa y^+. In Figure 12a the ordinate is the ratio of Reynolds to total shear stress, $\phi = <uv>/u_T^2(1-\xi)$, which is, of course, the ratio of turbulent to total (viscous plus turbulent) axial momentum transport in the radial direction; too, in the wall region under consideration, ξ is small so the total shear stress is close to T_w. The solvent ϕ profile is indicated by the broken line, but unfortunately Logan reported no solvent Reynolds stress data closer to the wall than $y^+ = 65$ so the region $10 < y^+ < 65$ is based on results of Laufer (1954) and Bremhorst and Walker (1973) at comparable R^+. In polymer solution, the data scatter considerably and therefore average values over various y^+ extents have been indicated by steps on the figure. For $10 < y^+ < 80$, ϕ in the polymer solution is less than in solvent, whereas for $y^+ > 80$ it is much the same as in solvent. In Figure 12b, the ordinate is the *u-v* correlation coefficient C_{uv} with values computed from the experimental Reynolds stress data of Figure 12a and the axial and radial intensity data of Figure 11a. The broken line represents solvent, and the polymer solution data have been averaged as in Figure 12a. It will be noticed that for $20 < y^+ < 80$ the value of $C_{uv} \simeq 0.2$ in the polymer solution is very significantly less than that in solvent, $C_{uv} \simeq 0.44$, whereas for $y^+ > 80$ values of $C_{uv} = 0.4 \pm 0.1$ in the polymer solution are much the same as in solvent. The observed decrease in C_{uv} in the wall region during drag reduction suggests that the polymer molecules reduce turbulent transport by decoupling the axial and radial velocity components rather than by suppressing the intensity of turbulence.
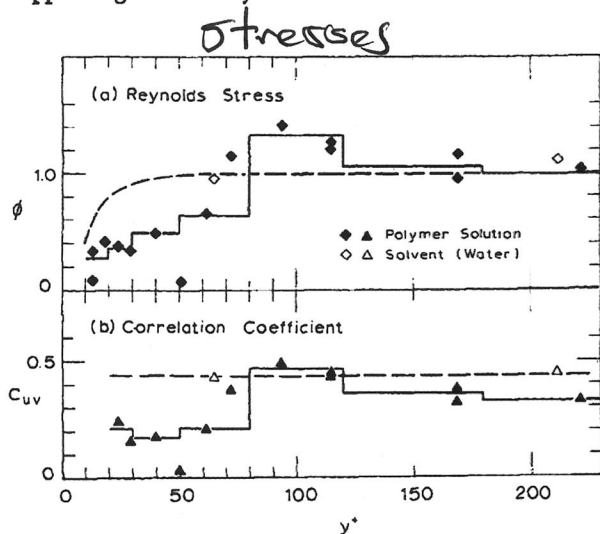

Fig. 12. Wall region profiles of (a) the ratio of Reynolds to total shear stress and (b) the u-v correlation of coefficient during drag reduction. Data of Logan (1972).

1.3.3 Turbulence Structure Zones. The axial intensity profile, for which the most information exists, has three zones:

1. A region $0 < y^+ < y_v^+$, say, in which α^+ and the magnitudes of u'^+ are essentially the same as Newtonian.

2. A region $y_v^+ < y^+ < y_e^+$, say, which is characteristic of drag reduction and in which u'^+ differs from Newtonian, being higher. This region further consists of a relatively thin portion, $y_v^+ < y^+ < y_{max}^+$, in which u'^+ increases to a maximum value and the remaining major portion $y_{max}^+ < y^+ < y_e^+$ in which u'^+ decreases from the maximum to a value close to Newtonian.

3. A region $y^+ > y_e^+$ or $1 > \xi > \xi_e$ in which u'^+ is the same as Newtonian.

The radial intensity, Reynolds stress, and correlation coefficient profiles do not yield information on the very near wall region (1) but do show clearly the region (2), toward the wall, which differs from Newtonian (v'^+, ϕ, C_{uv} are all relatively lower) and region (3), toward the axis, which is much the same as Newtonian.

There is evidently a striking analogy between the above turbulence structure zones and the (1) viscous sublayer, (2) elastic sublayer, (3) Newtonian plug zones of the mean velocity profiles considered earlier.

2. CORRELATION AND ANALYSIS

The object of this section is to correlate drag reduction data, using the elastic sublayer model (Virk, 1971) as a framework. The model is briefly described and then empirically related to experimental gross flow, mean velocity, and turbulence measurements with analysis and discussion of the data used for this purpose, including a section on polymer characterization. The empirical developments are, of course, substantially model independent.

2.1 The Elastic Sublayer Model

The essential physical notion is that the stimulation of polymer molecules by a turbulent shear flow creates a zone, called the *elastic sublayer*, which is characteristic of the drag reduction phenomenon. The elastic sublayer originates at onset, it then grows with increasing drag reduction and eventually occupies the entire pipe cross section at maximum drag reduction. By hypothesis, all drag reduction observations can be related to the properties and extent of the elastic sublayer.

The mean flow model is shown schematically in Figure 13, which defines all terminology. The general profile ABCD, consists of three zones: (1) a viscous sublayer AB, $y^+ \leqq y_v^+$; (2) an elastic sublayer BC, $y_v^+ < y^+ < y_e^+$; (3) a Newtonian plug CD, $y_e^+ \leqq y^+ \leqq R^+$, each with the indicated mixing length constant and U^+-y^+ relationship. The inner edge B of the elastic sublayer stays fixed at $y_v^+ = 11.6$, which is the trisection of Equations (7), (8), and (9), while its outer edge C moves along the ultimate profile BM from y_v^+ at zero drag reduction to R^+ at maximum drag reduction. Comparison of Figure 9 with Figure 13 shows that the model reproduces the essential features of the experimentally observed mean velocity profiles. The effective slip is related to elastic sublayer thickness by

$$S^+ = (A_m - A_n) \ln (y_e^+/y_v^+) \qquad (13)$$

Integration of the profile ABCD by segments yields the friction factor relations:

$$U_{av}^+ = A_n \ln R^+ + B_n - 1.5 A_n \quad ; \quad y_e^+ \to y_v^+ \qquad (14a)$$

$$= A_n \ln R^+ + B_n - 1.5 A_n$$

$$+ (A_m - A_n) \ln (y_e^+/y_v^+); \; y_v^+ < y_e^+ < R^+ \qquad (14b)$$

$$= A_m \ln R^+ + B_m - 1.5 A_m \quad ; \quad y_e^+ \to R^+ \qquad (14c)$$

— on drag reduction flows with
$\langle \tilde{u} \tilde{v} \rangle$

$\tilde{u}$ drops , $\tilde{v}$ increases.

↓   ↓
cross-stream   axial

— $R_g < l_d$ for all cases!

② { What is a Polymer ?
    { How does it behave in dilute
    { solution ?

(N.B. Dodges most of the really
interesting questions in polymer physics
i.e. gels, reptation, ...)

key: ■ Resonances of Polymer Chain

⇒ Approach via scaling laws ......

What is a Polymer (Chain) ?

— N >> 1 molecules in a long chain

$N \sim 10^5 - 10^6$.   structure: { linear, grid
                                       { branch
                              ↓
                    relevant ⟷ resist
                                    degradation
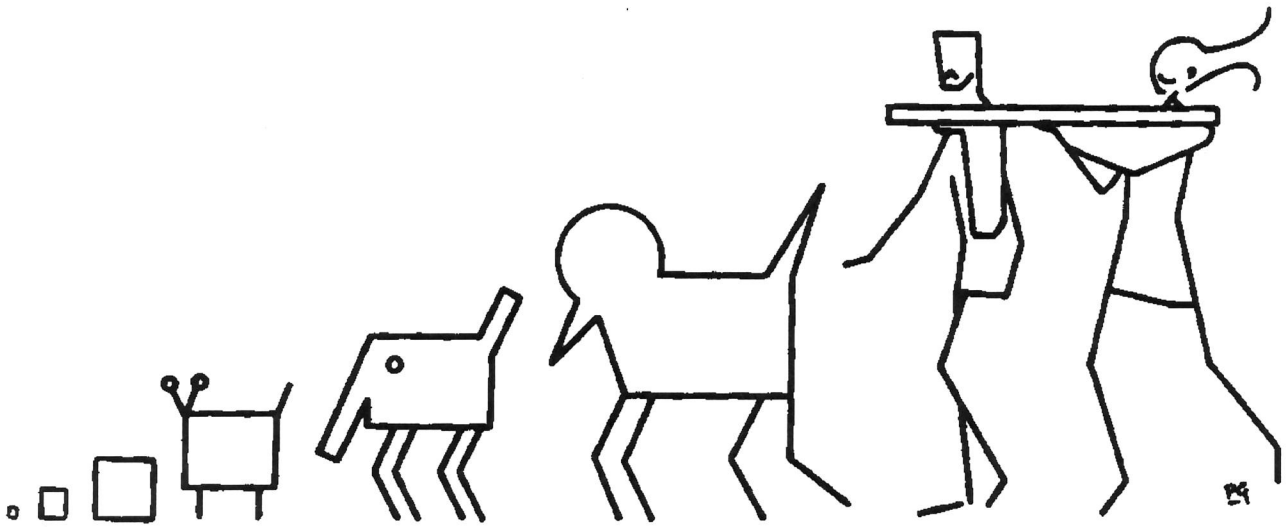
Various animals attempting to follow a scaling law.

de Gennes

i.e. polyethylene

$$-CH_2-CH_2-CH_2- \cdots \cdots \quad - \quad plastic$$
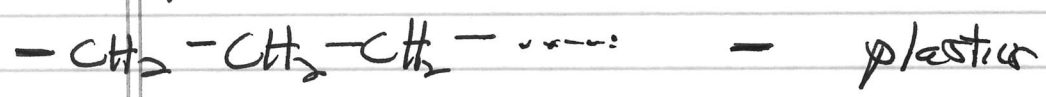
Polystyrene
(styrofoam)   — packing peanuts

$$-CH_2-CH-CH_2-CH$$
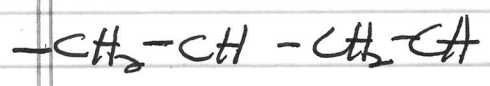
polyvinyl chloride (PVC)   — plastic pipes

$$-CH_2-CH-CH_2-CH$$
$$\quad\quad\quad | \quad\quad\quad\quad\quad\quad |$$
$$\quad\quad\quad Cl \quad\quad \blacksquare \quad\quad Cl$$
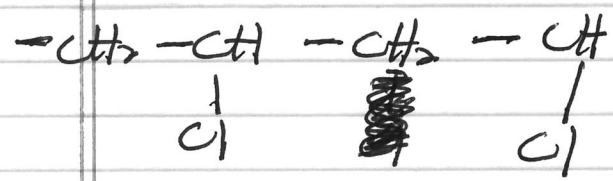
polyethylene dioxide (polyox) — common
drag-reduction
additive

Physically: — system is long chain
of monomer, with $N \sim 10^5$

— can be pure or in solution

— can add chemical agent to
change connectivity
(i.e. sulpher in vulcanization).

− Issues: (✳) − radius, scalings (with N)?
(how big?)

+++++ →
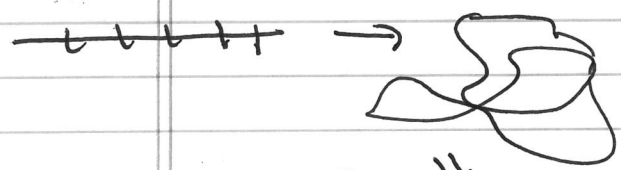
(✳) − "elasticity"? (drag reduction
⇔ coupling to
internal dofs

(✳) − natural modes ⇔
frequencies, relaxation rates.

− transport, material properties.

Some Basics:

− ideal chain { N monomers
{ spacing a

so # distinct conformations, or walks
starting from $\underline{r} = 0$ and ending at
$\underline{r}$ is $\Omega(\underline{r}) \to$ defin

− $\underline{r} = \underline{a_1} + \underline{a_2} + \underline{a_3} + \cdots \underline{a_N} = \sum_i \underline{d_i}$

each step uncorrelated, CLT ⇒
↳ mean square

$$\langle r^2 \rangle \sim N a^2$$
↑   ↳ #steps
avg (ms)
end−to−end dist

so Probability of extending to distance r is then

$$P(r) = \frac{\Omega(r)}{\sum_r \Omega_N(r)} \sim \frac{1}{N^{3/2}} \exp\left[-\frac{3r^2}{2}/Na^2\right]$$

$$P(r) \sim \frac{1}{N^{3/2}} \exp\left[-\frac{3}{2}r^2/Na^2\right]$$

to prob distr

and then can immediately write entropy, at elongation r

$$S = \ln(P(r)) = \ln \Omega(r)$$

$$\approx S(0) - \frac{3}{2}r^2/R_G^2$$

↳ radius gyration

$$R_G^2 = Na^2 \equiv (radius)^2 \text{ of polymer ideal chain}, \quad R \sim N^{1/2}$$

— radius is radius of walk of N steps

but $\quad F = E - TS \quad \equiv$ Helmholtz free energy.

∞

$$F = -k_BT \ln Z$$

$$F(r) = F(0) + \frac{3}{2} T r^2 / R_G^2$$

— free energy of ideal chain

— note entropy decreases but free
  energy increases, as chain extended.

i.e. $F(r) \cong U(r)$, $\qquad \not{F} = -\frac{\partial F}{\partial r} = -3T \frac{r}{R_G^2}$
  (eff potential)

Force

$$\boxed{k_{eff} = \frac{3T}{R_G^2} \equiv \text{entropic spring constant} \atop \text{of ideal chain}}$$

$\Longleftrightarrow$ Hookean elasticity via
  entropy.

Aside:
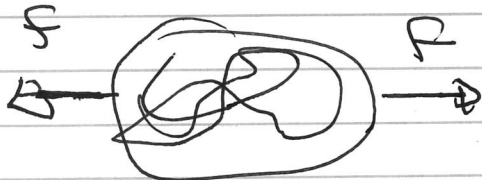
polymer pulled
at both ends by
force f.

elongation ??

— f $\Longleftrightarrow$ tension — const. along chain

$\langle r \rangle \sim N$ (linear scaling)

— expect $\langle r \rangle$ to depend on f, T, R_G

now $\sim f$. so

$$\langle r \rangle \sim (F R_G / T)^\alpha \ ? \quad \text{dimensionsly}$$

dim-less

$$\Rightarrow \quad \langle r \rangle \sim R_G (F R_G / T)^\alpha$$

and

$$\langle r \rangle \sim N \qquad \text{while} \quad R_G^2 \cong N a^2$$

$\therefore \quad \underline{\alpha = 1}$

and

$$\boxed{\langle r \rangle \sim F R_G^2 / T}$$

But:

— light scattering experiments suggested

$$R_G \sim N^{.6}$$

— Polymer is S A W → Self
   Avoiding Random Walk   (SAW)

   → effective monomer-monomer repulsion
   → chain swells'

   i.e. $R_G \sim N^{.6}$ vs $N^{1/2}$

How understand simply? (Too simply?)

→ explore competition:

① — exclusion/repulsion   (swelling)

② — contraction due entropic force

(after Flory)

→ chain monomer concentration
$\hookrightarrow$ dim

$$C \cong N/R^d$$

strong dimension sensitivity of walk crossing sens. to dim

$$F = F_{elastic} + F_{repul}$$

$$F_{elastic} \sim TR^2/kNa^2$$

$\hookrightarrow$ excluded volume factor.

$$F_{rep} \sim \frac{1}{2} T V(T) C^2 [R^d]$$

$\sim$ d-dim volume

$C-C$ repulsion

$$C = \frac{N}{R^d}$$

$$F \cong TR^2/kNa^2 + \frac{1}{2} T V(T) N^2/R^d$$

$$\frac{\partial F}{\partial R} = \frac{TR}{Na^2} - d\frac{TV(T)N^2}{R^{d+1}} = 0$$

has min

so $\quad R^{d+2} \sim V(T) N^3 a^2$

$R \sim R_F \sim N^{3/d+2} \left[a^2 V(T) \right]^{1/d+2}$

$\Downarrow$

Flory
predicting

$$\boxed{R_F \sim N^{3/d+2}}$$

$R_F \sim N^{.6} \checkmark$
$d=3$

$d=4 \Rightarrow RW \checkmark$

Note:

$\rightarrow$ simple but a swindle i.e.
mean field theory

① – repulsive energy over-estimated
 – neglects flctns $\langle \tilde{c} \tilde{c} \rangle$

② elastic energy over- estimated

$$1/R^2 \rightarrow 1/R_F^2$$

errors cancel!
Still
$\Rightarrow$ Simple Flory argument was a major
step forward on SAW understanding!

deGennes on Flory: " Simple ~~and~~ and brilliant
scheme"

→ How describe dynamics of chain ?

⇒ simplest approach is to view chain "as one of individual beads each feeling"

     — spring (entropic) force from neighbors

     — drag force on fluid

$n-1$ $n+1$ $n-2$
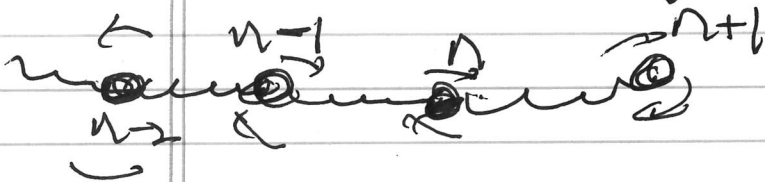
Rouse Model

$$m \ddot{\underline{r}}_n + \frac{1}{\mu} \dot{\underline{r}}_n = F_n$$

     neglect inertia

     drag on n^{th} bead.

     elastic force

$$\left\{ \begin{array}{l} \mu^{-1} = 6 \pi \eta \, a_* \\ \\ f_{drg} = 6 \pi \eta \, a_* \, \underline{V} \end{array} \right.$$

$$\frac{\underline{V}}{r_n} = \dot{\underline{r}}_n$$

Stokes.

$$\underline{f}_n = k \left[\underline{r}_{n+1} - 2 \underline{r}_n + \underline{r}_{n-1} \right]$$

     as usual.

so

$$\dot{\underline{r}}_n = \frac{T\mu}{a^2} \left[\underline{r}_{n-1} - 2\underline{r}_n + \underline{r}_{n+1} \right]$$

$\begin{cases} \text{drag} \\ \text{diffusive counterpart of HW pblm.} \end{cases}$

$ka \ll 1$

usual expansion

$$\Rightarrow \quad \dot{\underline{r}}_n = \frac{T\mu}{a^2} \frac{\partial^2 \underline{r}_n}{\partial n^2}$$

with free end:

$$\frac{\partial \underline{r}_n}{\partial n} \bigg|_{0,N} = 0$$

$$\boxed{1/\tau_p \sim \frac{p^2}{N^2} \frac{T\mu}{a^2}}$$

relaxation time of pth mode.

$$\boxed{1/\tau_1 \sim \frac{T\mu}{N^2 a^2} \sim \frac{T}{\boxed{N^2} 6\pi\eta a^3}}$$

$\mu \sim 1/6\pi\eta a_{hydro} \sim 1/\eta a.$

$$\boxed{\tau_p \sim N^2/p^2}$$

Now, Rouse model overlooks
hydro interference
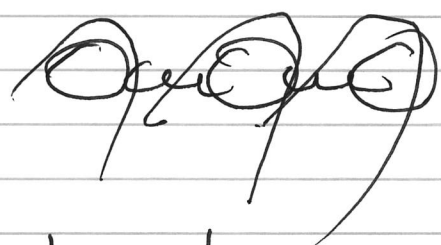
$\Rightarrow$ better $\perp$ elastic shape!

ℓ = length.
Polymer

$F = F_{drag} + F_{spring}$

$F_d = -6\pi \eta R_F \dfrac{d\ell}{dt}$

$F_{spr} \cong T\dfrac{\ell}{R_F^2}$

$0 = 6\pi \eta R_F \dfrac{d\ell}{dt} + \dfrac{T\ell}{R_F}$

$\Rightarrow$ $1/\tau_{damp} \sim T/6\pi \eta R_F^3$

$\tau_d \sim N^{9/5}$ for shape

vs. $\sim N^2$ for Rouse.

$\tilde{T}_d \equiv$ Zimm time

$\Rightarrow$ characteristic relaxation time of polymer b

$$\boxed{1/\tau_z \sim T/6\pi\eta R_F^3}$$

obviously, $\quad \dfrac{V(\ell)}{\ell} \quad$ vs $\quad 1/\tau_z$

is activation criterion.

TBC ....

(III)

→ Some Prevailing Wisdom
 (Lumley, DeGennes — see posted
  papers)

{ Lumley → pipe only
  deGennes → effect on cascade

— wall stress threshold.

$$\exists \ \ell \geq \ell_a \ \ \sigma/t$$

$$\frac{v(\ell)}{\ell} > 1/\tau_z$$

$$(\varepsilon/\nu)^{1/2} > 1/\tau_z$$

$$\varepsilon \equiv u_*^3 / \chi \quad \text{in pipe}$$

$$\rightarrow u_*^3 / a \ , \text{ macroscopically.}$$

and
$$\tau_w \sim \rho \, u_*^2$$

$\Rightarrow$ threshold $\text{vs } 1/R_F^3 \sim N^{-9/5}$

  emerges easily.

$\rightarrow$ larger polymers more easily
  activated.

– Drag Reduction

→ difficult to see substance.

→ <u>Lumley</u>

⇒ polymers stretch, damp turbulence.

⇒ how ??

coil-stretch transition rests on laminar extensional flow. Ċ dependence ?

~~HOW~~

→ DeGennes — see '86.

— activation

— cascade <u>truncation</u>   (?)

due to coupling to elastic DOFs

        elongate

— Ċ emerges via equipartition condition for truncation (?)

⇒ why truncation ?

(III.) A Model

→ Continuum 'Dumbell Model'

— seek a continuum model of Poly-Hydro
   turbulence

— exploit dumbell model ⟶ virtue of simplicity

⇒ what are effects of (minimal)
   elasticity on hydro interactions, cascade,
   transport, etc.?

⇒ Collective dynamics!?   (variant of
                                  FENE-B)

$$\underline{\underline{v}(r_1,t)} \qquad \underline{R} \qquad \underline{v}(r_2,t)$$

$$r_1 \qquad \qquad \qquad \qquad r_2$$
$$\longleftarrow \quad q \quad \longrightarrow$$
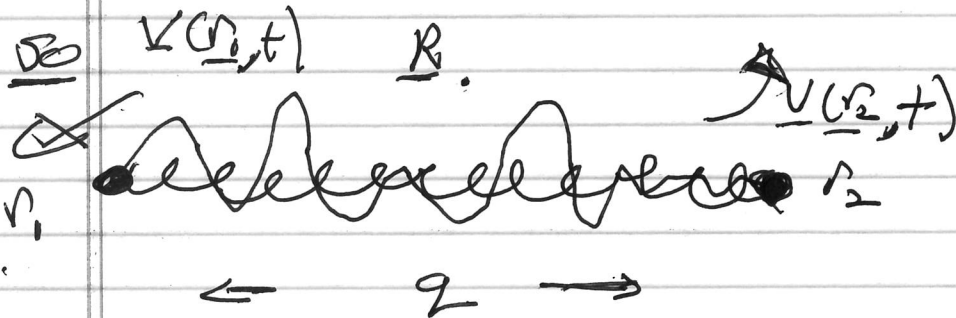
seek description in terms distribution
of $\underline{q}$ → relative coordinate

   $\underline{R}$ → centroid coordinate

and their distribution.

Now, the dumbells (i.e. shape elements)
go with the flow!

1

$$\gamma = 1/\mu$$

Langevin Eqns

$$\gamma\left(\frac{dr_1}{dt} - \underline{V}(\underline{r}_1, t)\right) = -\frac{\partial U}{\partial \underline{r}_1} + \frac{\Xi_1}{\uparrow}$$

$\uparrow$ drag

$\uparrow$ Entropic spring force

noise

and

$$\gamma\left(\frac{dr_2}{dt} - \underline{V}(\underline{r}_2, t)\right) = -\frac{\partial U}{\partial \underline{r}_2} + \Xi_2$$

$$U = \frac{1}{2} k \left(\underline{r}_1 - \underline{r}_2\right)^2$$

$\uparrow$ entropic

$$\langle \Xi_i(t) \Xi_j(t') \rangle = 2\gamma k_B T \delta_{ij} \cdot \delta(t - t') \quad \text{—usual}$$

Then:

$$\underline{R} = \frac{1}{2}\left(\underline{r}_1 + \underline{r}_2\right) \quad \rightarrow \text{centroid}$$

$$\underline{q} = \underline{r}_1 - \underline{r}_2 \quad \rightarrow \text{extension.}$$

so , can write Langevin Eqns. as:

$$\frac{dR}{dt} = \underline{V}(\underline{R}, t) + \frac{1}{2\gamma}\left[\Xi_1(t) + \Xi_2(t)\right]$$

extension.   N.B. : A hint as to
   ↓   where fluid equations
                  come from.

$$\frac{d\underline{z}}{dt} = \underline{z} \cdot \underline{\nabla} \, \underline{v}(\underline{R}, t) - \frac{2}{\gamma} \frac{\partial u}{\partial \underline{z}}$$

$$+ \frac{1}{\gamma} \left[\underline{\xi}_1(t) - \underline{\xi}_2(t) \right]$$

Now, to derive fluid equations for polymer DOF, need kinetic equation for:

$$F(\underline{z}, \underline{R} \mid \underline{v} \ldots \text{etc})$$
      ↑
distribution of polymer DOFs.

∂/∂   have Fokker-Planck equation

$$\frac{\partial F}{\partial t} = -\frac{\partial}{\partial \underline{R}} \left[\underline{v}(\underline{R}, t) \, F \right]$$

$$+ \frac{\partial}{\partial \underline{R}} \cdot D_0 \frac{\partial}{\partial \underline{R}} F$$

$$- \frac{\partial}{\partial \underline{z}} \cdot \left[\underline{z} \cdot \underline{\nabla} \underline{v}(\underline{R}, t) - \frac{2}{\gamma} \frac{\partial u}{\partial \underline{z}} \right]$$

$$+ \frac{\partial}{\partial \underline{z}} \cdot D_z \frac{\partial F}{\partial \underline{z}}$$

where: $D_0 = k_B T / 2\gamma$

$$D_z = 2 k_B T / \gamma$$

and $\qquad \int d^3\underline{R} \int d^3\underline{z} \; F(\underline{R}, \underline{z}, t) = I$

Now, take moments:

$$c(\underline{R}, t) = \int d^3\underline{z} \; F(\underline{r}, \underline{z}, t)$$

↓
concentration
of polymers/
dumbells

and

$$\underline{Q}(\underline{R}, t) = \int d^3\underline{z} \; \underline{z} \; F(\underline{r}, \underline{z}, t)$$

$\llcorner\rightarrow$ (naively) the natural
order parameter.

$\overline{\underline{v}_0}$

$$\frac{\partial c}{\partial t} = \int d^3\underline{z} \; \frac{\partial f}{\partial t}$$

$$= -\underline{v} \cdot \underline{\nabla} c + D_0 \nabla^2 c$$

⇏

$$\boxed{\frac{\partial c}{\partial t} + \underline{v} \cdot \underline{\nabla} c = D_0 \nabla^2 c}$$

as $\underline{\nabla} \cdot \underline{v} = 0$.

in homogeneous turbulence:

$$c(\underline{R}, t) \rightarrow c_p \sim \text{const.}$$

Now, consider elongation moment:

$$\underline{\Psi}(\underline{R},t) = \int d^3 \underline{z} \ \underline{z} \ F(\underline{R},\underline{z},t)$$

$$\int d^3 \underline{z} \ \underline{z} \left[\underbrace{\frac{\partial F}{\partial t}}_{①} + \underbrace{\frac{\partial}{\partial \underline{R}} \left(\underline{v}(\underline{R},t) F \right)}_{②} \right]$$

$$+ \underbrace{\frac{\partial}{\partial \underline{R}} \cdot D_0 \cdot \frac{\partial F}{\partial \underline{R}}}_{③}$$

$$= \int d^3 \underline{z} \ \underline{z} \left[\underbrace{-\frac{\partial}{\partial \underline{z}} \left(\underline{z} \cdot \nabla \ \overline{\underline{v}} F \right)}_{④} - \underbrace{\frac{\partial}{\partial \underline{z}} \cdot \frac{2}{\gamma} \frac{\partial \underline{k} F}{\partial \underline{z}}}_{⑤} \right]$$

$$+ \underbrace{\int d^3 \underline{z} \ \underline{z} \ \frac{\partial}{\partial \underline{z}} \cdot D_z \frac{\partial F}{\partial \underline{z}}}_{⑥}$$

$$\begin{bmatrix} \text{note: Closure problem} \\ \text{if non-Hookean spring} \end{bmatrix}$$

So

$$\underbrace{\frac{\partial \underline{\Psi}}{\partial t}}_{①} + \underbrace{\underline{v} \cdot \nabla \underline{\Psi}}_{②} = \underbrace{D_0 \nabla^2 \underline{\Psi}}_{③} + \underbrace{\underline{\Psi} \cdot \nabla \underline{v}}_{④}$$

$$\underbrace{-\frac{2k}{\gamma} \underline{\Psi}}_{⑤} + \underbrace{\diagup}_{⑥}$$

note $\dfrac{k}{\gamma} = \omega_z \quad \Rightarrow$ Zimm frequency / relaxation rate

$$k = \frac{T}{R_G^2} \quad , \quad \gamma = 6\pi \eta_s R_G$$

$$\omega_z = T / 6\pi \eta_s R_G^3 \qquad\qquad R_G = R_F.$$

thus, have:

$$\frac{\partial \underline{\varphi}}{\partial t} + \underline{v} \cdot \underline{\nabla} \underline{\varphi} = \underline{\varphi} \cdot \underline{\nabla} \underline{v} - 2\omega_z \underline{\varphi} + D_B \nabla^2 \underline{\varphi}$$

where ② , ③ , ④ label the terms.

② → advection

③ → stretching

④ → Zimm relaxation damping
    → scale invariant.

n.b. ∴ Obvious similarity to
      conduction equations:

$$\frac{\partial \underline{\omega}}{\partial t} = \underline{\nabla} \times \underline{v} \times \underline{\omega} + \nu \nabla^2 \underline{\omega}$$

$$\frac{\partial \underline{B}}{\partial t} = \underline{\nabla} \times \underline{v} \times \underline{B} + \eta \nabla^2 \underline{B}$$

③ → stretching
    i.e. flow strains stretch the
         polymer

④ → Zimm damping → resists stretching
    i.e. scale invariant relaxation
         rate.

are key terms.

N.B. As anticipated

$$|\nabla \underline{V}| > \omega_z$$

"required for
"polymer activity".

Is this correct ??

$\rightarrow$ NO

$\rightarrow$ Direction of stretching field
not established.

Points 1, 2 arbitrary !

$\underline{Q}$, $-\underline{Q}$ equally likely.

$\Rightarrow$ Polymer tension better thought of
as a dyad $\leftrightarrow$ tensor

not $\uparrow \underline{B}$ but $\updownarrow Q_{ij}$

has direction
and tension.

($if \hat{b} \cdot \nabla \hat{b} \neq 0$)

has no direction
but has tension

→ Akin to order parameter for nematic liquid crystals

so better and meaningful order parameter
if:

$$Q_{ij}(\underline{R}, t) = \int d^3 z \; z_i z_j \, f(\underline{R}, \underline{z}, t)$$

↓
elastic energy field   (akin energy
                                         tensor)

<u>N.B.</u> Elastic energy tensor is natural
for weak field MHD (small)
scale dynamo, etc.

so

$$\partial_t Q_{ij} + \underline{V} \cdot \underline{\nabla} Q_{ij}$$
②

$$= Q_{iy} \partial_y V_j + Q_{jr} \partial_r V_i - 4\omega_z Q_{ij}$$
③   ④

$$+ D_0 \nabla^2 Q_{ij} + \frac{4 k_B T}{\gamma} \delta_{ij}$$
⑤

Physics picture essentially unchanged

② → advection

③ → stretching, need symmetrize

④ → Relaxation damping

③ Noise → thermal levels of excitation.

For equilibrium   (Do feeble)

$$-4\omega_z Q_{ij} + 4\frac{k_B T}{\gamma}\delta_{ij} \simeq 0$$

$$Q_{ij} \simeq \delta_{ij} \frac{k_B T}{k}$$

$$\simeq R_G^2 \delta_{ij}$$

Back Reaction on Fluid

Observe, then Q_{ij} as elastic energy field, naturally suggests writing back-reaction as $\underline{\nabla} \cdot \underline{\underline{\sigma}}$ on RHS of N-S:

c.e.

$$\rho\left[\frac{\partial \underline{v}}{\partial t} + \underline{v}\cdot\underline{\nabla}\,\underline{v}\right] = -\underline{\nabla}p + c_p \overset{\text{spring const}}{\overset{\Downarrow}{k}}\,\underline{\nabla}\cdot\underset{\underset{\text{concentration field}}{\Uparrow}}{\underline{\underline{\varphi}}} + \eta\,\underline{\nabla}\,\underline{v}$$

more precise: $\underline{\underline{\sigma}} = c_p k\,\underline{\underline{\varphi}}$
                 $\underset{\underset{\text{stress tensor}}{\Uparrow}}{}$

In component form:

$$\rho \left[\partial_t V_i + \underline{V} \cdot \underline{\nabla} V_i \right] = - \nabla_i P + \nabla_j \tau_{ij}$$

$$+ \mu \nabla^2 \underline{V_i}$$

— obvious analogy

elastic stress : $\tau_{ij} \cong E \left(\underline{\nabla} \underline{\Sigma} \right)$

$\Rightarrow$ elastic waves $\qquad \partial_t^2 \underline{\Sigma}$

Polymer stress $\tau_{ij} = c_p k \, \mathbb{Q}_{ij}$

$\Rightarrow$ ⓐ elastic waves (akin Alfven)

so, with Polymer fluid is both

viscous and elastic

i.e.

$\underline{\tau} = c_p k \, \mathbb{Q}_{ij} \quad , \quad -\mu \underline{\nabla} \underline{V}$

(beware different sign
conventions)

and note if linearize $\mathbb{Q}_{ij}$

$$\partial_t \tilde{Q}_{ij} = Q_{ir} \partial_r V_j$$

$$\rho \, \partial_t \tilde{V} = \nabla_j C_p k \tilde{Q}_{ij} +$$

$$\Rightarrow \rho \, \partial_t^2 \tilde{V}_i = \nabla_j C_p k \partial_t \tilde{Q}_{ij}$$

$$= \nabla_j C_p k Q_{ij}^{(l)} \partial_r V_j$$

$\Rightarrow$ suggestive of elastic wave response, due polymer.

of course,

$$\partial_t \underline{V} = \eta \, \partial^2 \underline{V} \qquad\qquad viscous.$$

Welcome to "viscoelasticity", a property of polymeric fluids!

N.B.   A close correspondence exists between:

Classes of polymer·hydro models
$\Longleftrightarrow$ MHD   (evident)

Classes of viscoelastic systems
(Oldroyd-B) $\Longleftrightarrow$ MHD
see Ogilvie + Proctor   "

Physics of back-reaction:
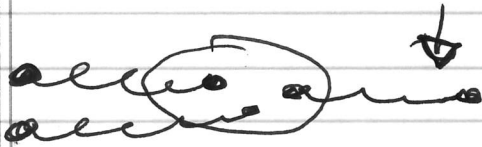
$\uparrow$ fluid element

$\downarrow$ dumbells
piercing surface of
the dumbell.

So, the Poly-Hydro system:

$$\partial_t Q_{ij} + (\underline{v} \cdot \underline{\nabla}) Q_{ij} = Q_{iy} \partial_y V_j$$

$$+ Q_{cy} \cancel{\partial_j V_y} - 4 \omega_z Q_{ij} + D_o \nabla^2 Q_{ij}$$

$$+ \frac{4 T_{hb}}{\gamma} \delta_{ij}$$

and

$$\rho \left[\frac{Dv_i}{Dt} + \underline{v} \cdot \underline{\nabla} V_i \right] = -\nabla_i P_i + \partial_j c_p k Q_{ij}$$

$$+ \mu \nabla^2 V_i + f_i$$

$\downarrow$ forces,

$\rightsquigarrow$ Regarding energetics:

$$E = \frac{1}{2} \int d^3r \left[\rho v^2 + c\rho k \, Q_{kk} \right]$$

conserved to:

$$\frac{dE_{Tot}}{dt} = -\int d^3r \left[\rho \nu (\partial_i v_j)^2 + 4 \omega_g \, Q_{kk} \right]$$

Do irrelevant.

N.B. Obvious closer analogy with
__MHD__

$$\partial_t \underline{B} = \underline{\nabla} \times (\underline{v} \times \underline{B}) + \eta \nabla^2 \underline{B}$$

$$\left[\partial_t \underline{B} + \underline{v} \cdot \underline{\nabla} \underline{B} = \underline{B} \cdot \underline{\nabla} \underline{v} + \eta \nabla^2 \underline{B} \right.$$

→ obviously no counterpart of Zimm damping in MHD

and

$$\rho \frac{dv}{dt} = -\underline{\nabla} P + \frac{\underline{J} \times \underline{B}}{c} + \rho \nu \nabla^2 \underline{v}$$

idea $\frac{\underline{J} \times \underline{B}}{c}$ + Ampere ⟹

$$\rho\left(\frac{\partial V}{\partial t} + \underline{V} \cdot \underline{\nabla} \underline{V}\right) = -\underline{\nabla} p^+ + \frac{\underline{B} \cdot \underline{\nabla} \underline{B}}{4\pi} + \eta \nabla^2 \underline{B}$$

$\underline{\nabla} \cdot \underline{B} = 0$ can write as $\underline{\nabla} \cdot \left[\dfrac{\underline{B}\,\underline{B}}{4\pi}\right]$

N.B.   A key element in incompressible MHD is the Alfvén wave

Fermi: "Magneto - elastic wave"

$$\underline{\nabla} \cdot \underline{V} = 0 \qquad\qquad \underline{B} = B_0 \hat{z}$$

$$\rho_0 \, \partial_t \, \underline{\tilde{V}} = -\underline{\nabla} p^+ + \frac{B_0 \partial_z \underline{\tilde{B}}}{4\pi}$$

$$\frac{\partial \underline{\tilde{B}}}{\partial t} = B_0 \partial_z \underline{\tilde{V}}$$

so $$\omega^2 = \left(\underline{k} \cdot \underline{b_0}\right)^2 B_0^2 \Big/ 4\pi \rho_0$$

$$= k_{||}^2 V_A^2$$

i.e. for incompressible MHD, with strt field, linear wave is excitation beie state

contrast: $\underline{\nabla} \cdot \underline{V} = 0$ hydro.
i.e. this course!

What of Poly-Hydro ?   Factorize:

so $Q_{ij} \simeq (Q_{0i} + \delta Q_i)(Q_{0j} + \delta Q_j)$ (o not énly)

$= Q_{0i} Q_{0j} + Q_{0i} \delta Q_j + \delta Q_i Q_{0j}$

$Q_0 \perp \delta Q$

$\Rightarrow$ usual :

$$\omega(\underline{k})^2 = \frac{c_p H}{c_0} (\underline{k} \cdot \vec{Q_0})^2$$

local field

$\rightarrow$ Alfvén - like elastic waves present

$\rightarrow$ More significantly :

With Alfvenic / elastic wave coupling,
turbulence character changes
fundamentally. As a reference pt.
MHD turbulence (weak magnetization)

$\rightarrow$ wave-like, or 'weak'

$\rightarrow$ wave interactions control
cascade, not eddy

$\rightarrow$ inertial range spectrum,
power transfer fundamentally
different from phys/les.

→ Mini – Primer on MHD Cascade

cf: 218b Notes
   S. Galtier "Modern MHD"
   R. McKilVened "Plasma Physics for Astrophysics"

→ $Z_{\pm} = \underline{V} \pm \underline{b}$ are exact, NL solutions

interaction only via $\ne$ – collisions   [Elsasser variables

→ basic physics is wave interaction
$\underline{\underline{us}}$ centered:

$$\epsilon = \frac{V(\ell)^2}{\tau(\ell)_{Tr}} \longrightarrow \frac{V(\ell)^2}{\tau(\ell)} = \frac{V(\ell)^3}{\ell}$$

$$\sim \quad \sim$$

have:

$$\epsilon = (C(\ell))^2 (Z(\ell)^2)^2 \tau_{Tc}$$

      ↓   ↓   ↓
  coupling   energy   wave interaction
  coeff.   coherence

akin $\dfrac{d\epsilon}{dt} = T \epsilon$
                    ↓
            transition rate

$$T = \sum |\langle \psi | V_{int} | \psi \rangle|^2 \pi \, \delta(E_{\psi} - E_{\psi} - \hbar \omega_{\psi})$$

→ strain field of
~~k~~ scattering wave packet

$$T \sim (\varepsilon(\ell))^2 \, z(\ell)^2 \quad \blacksquare \quad \tau_{T_c}$$

$$\sim \frac{1}{\ell^2} z(\ell)^2 \, \tau_{T_c}$$

$\tau_{T_c} \rightarrow$ interaction time

$$\sim (b_o / \ell)^{-1}$$

$$\rightarrow (V_{Arms} / \ell)^{-1} \qquad \rightarrow \text{wave packet passage}$$
$$\qquad \qquad \qquad \qquad \text{time, scale } \ell.$$

↑

Alfven
speed in   → local, produced
rms field   by stretching

∅

$$\boxed{ \varepsilon \approx \frac{1}{\ell^2} \frac{(z(\ell)^2)^2}{} \frac{\ell}{V_{A \, rms}} }$$

$$z(\ell) \sim (V_{A_o} \varepsilon)^{1/4} \ell^{1/4}$$

$$\Rightarrow \quad E_K(\ell) \sim E_M(\ell) \sim (\epsilon V_{A0})^{1/2} \ell^{1/2}$$

$$\boxed{E_K(k) \sim E_M(k) \sim (\epsilon V_{A0})^{1/2} k^{-3/2}}$$

$\sim$ Kraichnan - Iroshnikov Spectrum.

$$- \quad \frac{1}{\tau_{Tr}} \sim \frac{v}{\ell^2}$$

$$\frac{3(\ell)^2}{\ell^2} \tau_A \qquad\qquad \tau_A = \frac{\ell}{V_{A0}}$$

$\Rightarrow$ changes in dissipation scale ℓ_d, but $\underline{\text{no}}$ $\underline{\text{truncation}}$!

$\Rightarrow$ can argue on basis of analogy with MHD

$-$ in activated region (in $\underline{\text{scale}}$), $\qquad\qquad$ where ℓ^*, ℓ^{**}!

hydro cascade will convert to hydro / elastic cascade.

- spectrum} will be modified
  ld

- turbulence converted from
  hydro / k^{-41} to <u>elastic wave</u>
  turbulence, with

$$E_Q \sim E_k \qquad \rightarrow \text{\textcircled{ε}} \text{ equipartition of}$$
$$\text{kinetic, elastic DoF.}$$

$\Rightarrow$ (IV.) Yet More ...
Speculations on Drag Reduction:

- recall essence of drag is momentum
  transport to (no slip) wall.

- polymer activated if for $l > l_d$

$$\frac{V(l)}{l} > 1/\tau_z = \text{defines } l_z$$

$$\Rightarrow \epsilon^{1/3} \left(\frac{\nu^{3/4}}{\epsilon^{1/4}} \right)^{-2/3} > 1/\tau_z$$

$$\epsilon^{1/3} \frac{\epsilon^{1/6}}{\nu^{1/2}} = \left(\frac{\epsilon}{\nu} \right)^{1/2} > 1/\tau_z$$

so

— i.f.

Hydro

Poly active
ℓ^*

—Hydro–Elastic—— ℓ^{**} $\left\{\begin{array}{l}\text{not clear} \\ \text{single chain} \\ \text{analysis, à la de G,} \\ \text{carrier over.}\end{array}\right.$

ℓ_d

in hydro–elastic range, polymer DoF's can/may be stretched to ~ equipartition with kinetic energy.

for mean flow evolution in charteal layer.

— recall: Reynolds ← now elastic

$$\partial_t \langle V_{\shortparallel} \rangle = -\nabla_\perp \cdot \left\{ \langle V_\perp V_{\shortparallel} \rangle - \frac{c_p k}{2\Omega} \langle \underline{\underline{B}}_{\perp \shortparallel} \rangle \right\}$$

mean flow

note: total stress in activated region

now, if turbulence 'elasticized' (i.e. akin Alfvenized) → converted to elastic waves

then $\langle V_\perp V_{\shortparallel} \rangle \simeq \frac{c_p k}{2\Omega} \langle \underline{\underline{B}}_{\perp \shortparallel} \rangle$

<u>∞</u> can expect reduction in
<u>net stress</u> due kinetic-elastic
competition.

→ degree reduction will require/depend on
approach to equipartition.

→ obviously:

— higher C_p beneficial!

⟹ glimmer of concentration dependence
appearing

→ quantitative?

— hydro-elastic layer ⟹ buffer layer,
defined by transport reduction.

→ Problem now closely tracks
small scale dynamo problem at
large P_m! (tensor)

⟹ how close will hydro-elastic

⟹ what scale turbulence come to ① equipartition?

21

on elastic range ?

Other issues:

   — elastic effect on $\langle v_{\perp} v_{\parallel} \rangle$?
      cross phase $\Rightarrow$ $C[u, v]$

   — detailed differences between
      Hydro - elastic, MHD

but $\rightarrow$ $\underline{local}$ $\langle \phi \rangle$ $\hookleftarrow$ ϕ_{rms}

       seems compelling.

Subject open for further study and
contradiction ?